

Application of response surface methodology for thorium(IV) removal using Amberlite IR-120 and IRA-400 : Ion exchange equilibrium and kinetics

Ehsan Zamani Souderjani¹, Ali Reza Keshtkar^{2,*}, Mohammad Ali Mousavian¹

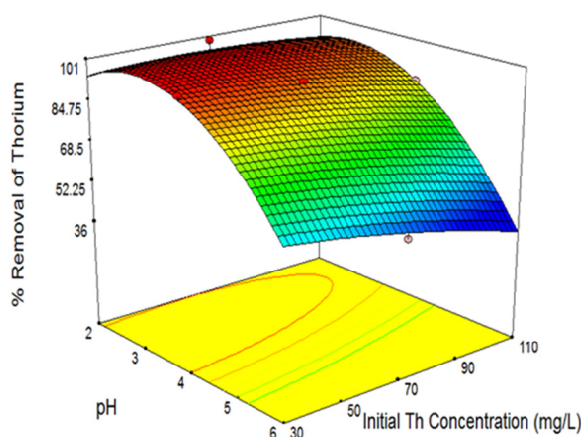
¹ Department of Chemical Engineering, Collage of Engineering, University of Tehran, Tehran, Iran

² Nuclear Fuel Cycle School, Nuclear Science and Technology Research Institute, Tehran, Iran

HIGHLIGHTS

- A novel PVA/TiO₂/ZnO/TMPTMS nanofiber adsorbent was fabricated by the electrospinning method.
- The effects of pH, initial Th(IV) concentration and the amount of adsorbent were investigated.
- The properties of the prepared novel adsorbent were determined by FTIR analysis.
- The adsorption capacity of Th(IV) in a single system was reported.
- The mechanism of Th(IV) adsorption was recognized.

GRAPHICAL ABSTRACT



ARTICLE INFO

Article history:

Received 13 June 2017

Revised 31 August 2017

Accepted 31 August 2017

Keywords:

Th(IV) removal

Response surface methodology (RSM)

Central composite design

Ion exchange resin

ABSTRACT

In this work, thorium(IV) removal from aqueous solutions was investigated in batch systems of cationic and anionic resins of Amberlite IR-120 and IRA-400. In this way, the effects of pH, initial Th(IV) concentration and the amount of adsorbent were investigated. A Central composite design (CCD) under response surface methodology (RSM) was employed to determine the optimized condition. The results showed that the maximum removal efficiency of Th(IV) onto IR-120 and IRA-400 either discretely or in combination, albeit with equal mass fraction, was determined as follows: 98.09%, 65.70% and 72.19% at pH=3.23, 6 and 4.07, initial Th(IV) concentration of 78.2, 30 and 55.4 mg.L⁻¹ and 2.08, 2.5 and 2.2 g.L⁻¹ of resin, respectively. The kinetic and equilibrium data were accurately described by the pseudo-second order and Langmuir models. The results showed that IR-120 is a suitable adsorbent for thorium removal from aqueous solutions.

* Corresponding author: Tel.: +9821-82064399 ; Fax: +9821-82064399 ; E-mail address: akeshtkar@aeoi.org.ir

DOI: 10.22104/jpsst.2017.2267.1088

1. Introduction

During the last century, thorium has been widely used in a variety of industries such as electronic equipment [1]. Thorium is a naturally occurring radioactive element which is distributed over the earth's crust. The toxic nature of this radionuclide has been a public health dilemma for many years, even at trace levels [2]. It must be mentioned that Thorium can affect human health by causing such diseases as lung and liver cancers [3,4]. Thorium nitrate mainly localizes in the liver, spleen and marrow and it may precipitates in a hydroxide form [5]. Thorium, uranium and other actinides also lead to irrecoverable damage to the environment [6]. Due to the above facts, the removal of Thorium from aqueous solutions is necessary and several methods have been proposed [7]. One of the easiest and consequently environmental friendly way to remove this element is by adsorption. Sorption using simple and cheap adsorbents is gaining a lot of importance and there is ongoing research for the development of newer, cheap and easily available sorbents to avoid regeneration [8,9].

Different types of materials have been used as adsorbents for thorium adsorption, such as activated carbons, zeolites [10], alumina, silica [11], crystalline tin oxide nanoparticles [12] and polyvinylalcohol/titanium oxide nanofiber [13], but to our knowledge there is no data on adsorption of thorium on Amberlite IR-120 and IRA-400.

Ion exchange is one of the most popular methods for the removal of metal ions from aqueous solutions [14]. The ion exchange process has been developed as a major option for separation of metals from aqueous solutions such as purification of wastewater. The hydrogen ions released from the cationic ion exchange resin neutralize the hydroxide ions. The influence of complex formation on ion exchange adsorption equilibrium and on the distribution of metal ions between the liquid and resin phase has been extensively studied [15-17]. Ion exchange resins are usable at different pH values and high temperatures. Also, they are insoluble in most organic and aqueous solutions. These resins contain a covalent bonding between the charged functional groups and the cross linked polymer matrix [18]. The practical application of ion exchange resins is in a continuous electro deionization (CEDI) system. In this process, the dilute compartment is occupied with ion exchange resins that enhance the transport of cations or

anions under the driving force of a direct current. In CEDI operation, hydrogen and hydroxyl ions were produced which regenerate the resins electrochemically without using any chemicals for regeneration [19]. The main advantages of this method are a higher recovery ratio and less pollution. This process has been adapted for the removal of sulfate, chloride and metal ions such as potassium, calcium and magnesium by using Amberlite IR-120 and IRA-400 [20-23]. Many studies have been reported on adsorption of metal ions using ion exchange resins such as Amberlite XAD-4 [24,25], IR-120 [26], CG-400 [27], and IRN-77 [28]. Recently, Singh *et al.* [29] studied the extraction of Thorium using ionic liquid based solvent systems.

In the recent studies the effect of individual parameters has been reported in order to maintain the other process parameters at unspecified levels. This approach can not consider the combined effect of all process parameters. Therefore, it requires a number of experiments to determine optimum levels, which may still be unreliable. Response surface methodology (RSM) can eliminate these limitations of a classical method by optimizing all the process parameters collectively by utilizing a statistical experimental design [30].

The aim of the present study is optimizing the removal of Th(IV) ions from aqueous solutions using resins of Amberlite IR-120 and IRA-400 in a batch mode. Central composite design (CCD) was used to determine the quantitative relationship between the response and the levels of the experimental factors. In the this work the effects of pH, initial Th(IV) concentration and adsorbent dosage on the adsorption process were investigated using this statistical design, and subsequently those levels were optimized.

2. Materials and methods

2.1. Materials

A strong basic anion exchange resin (Amberlite IRA-400 Cl) and a strong acidic cation exchange resin (Amberlite IR-120 Na) were purchased from BDH Chemical Co. Their properties are listed in Table 1. The solution of 100 mg.L⁻¹ of thorium was prepared from Th(NO₃)₄.5H₂O (98.5% purity, Merck Co.) by dissolving the salt in double distilled water. More diluted solutions were prepared daily as required. The pH of the solutions was adjusted using HNO₃ and NaOH. All the

experiments were carried out at 20 ± 2 °C.

2.2. Preparation of adsorbent

The cationic and anionic resins were initially immersed in HCl (10%) and stirred for 30 minutes, separately. After being rinsed twice with deionized water, the anionic resin was regenerated with NaOH solution (4%). The resins were again rinsed three times with deionized water, after that the cake was separated from water via filtration and finally dried completely at 60 °C.

2.3. Batch adsorption studies

The behavior of Th(IV) adsorption towards the cationic and anionic resins were examined in flasks containing 100 mL Th(IV) solution by shaking the flasks at 150 rpm at a period contact time of 15 h. Batch adsorption experiments were performed at room temperature (20 ± 2 °C) to study the effects of pH, initial Th(IV) ion concentration and the dosage of adsorbent on optimization of Th(IV) removal by CCD under RSM. The concentration of Th(IV) ion before and after equilibrium adsorption was measured utilizing an inductivity coupled plasma atomic emission spectrophotometer (ICP-AES, Thermo Jarrel Ash, Model Trace Scan). The adsorption capacity and metal removal were defined as follows [31]:

$$q_e = \frac{(C_0 - C_e)V}{m} \quad (1)$$

$$R = \frac{C_0 - C_e}{C_0} \times 100 \quad (2)$$

where q_e (mg.g⁻¹) is the equilibrium capacity and R is the metal adsorbed percentage by ion exchange resins; C_0 and C_e (mg.L⁻¹) are the initial and equilibrium metal ion concentrations, respectively; and V and m are the liquid volume (L) and the weight of dried used adsorbent (g), respectively.

2.4. Experimental design

Optimum conditions for the adsorption of Th(IV) by IR-120 and IRA-400 either discretely or in combination, albeit with equal mass fraction, were determined by means of CCD under RSM. The RSM consists of a group of empirical techniques to evaluate a relationship between a cluster of controlled experimental factors and measured responses due to one or more selected criteria. In this study the optimization was carried out by focusing on the effect of three variables including cationic and anionic resins dosages, initial Th(IV) concentration and pH. The independent variables used in this study were coded according to Eq. (3).

$$x_i = \frac{X_i - X_0}{\Delta X} \quad (3)$$

where x_i is the dimensionless coded value of the i th independent variable, X_i is the real value of the independent variable, X_0 is the value of X_i at the center point and ΔX is the step change value. The behavior of the system is defined by the following empirical second-order polynomial model [32]:

$$y = \beta_0 + \sum_{i=1}^z \beta_i X_i + \sum_{i=1}^{z-1} \sum_{j=1}^z \beta_{ij} X_i X_j + \sum_{i=1}^z \beta_{ii} X_i^2 + \epsilon \quad (4)$$

where y is the predicted response, β_0 is the intercept term, β_i is the linear effect, β_{ii} is the quadratic effect, β_{ij} is the interaction effect, X_i is the input variable affecting the response of y , X_i^2 is the square effect, $X_i X_j$ is the interaction effect and ϵ is a random error.

DESIGN EXPERT 7.0 (Stat-Ease, Inc, Minneapolis, MN, USA) software was utilized for graphical analysis and regression of the obtained data. In this way, a design of 20 experiments was formulated and then all variables were coded at five levels: $-\alpha$, -1 , 0 , $+1$ and $+\alpha$. Finally, the optimum values of the selected variables were found by solving the regression equation. The range and the level of these variables in coded values from RSM studies are given in Table 2.

Table 1. Properties of the cationic and anionic resins.*

Name	Matrix	Functional group	Total exchange capacity (eq.kg ⁻¹)	Harmonic mean size (mm)
Amberlite IR-120 Na	Styrene DVB copolymer	$R-SO_3^-$	$5 \geq$ of dry mass	0.62-0.83
Amberlite IRA-400 Cl	Polystyrene DVB	$-N^+R_3$	2.6-3 of dry mass	0.3-0.9

* Obtained from the manufacturer

Table 2. Experimental ranges and levels of the independent variables.

Independent variables	Range and level				
	$-\alpha$	-1	0	+1	$+\alpha$
pH (A)	2	3	4	5	6
Initial thorium concentration, mg.L ⁻¹ (B)	30	50	70	90	110
Adsorbent dosage, g.L ⁻¹ (C)	0.5	1	1.5	2	2.5

3. Results and discussion

3.1. Fitting the process models

The results are obtained with an experimental design aimed at identifying the best levels of the selected variables. The full factorial central composite design matrix of orthogonal and real values of adsorbent dosage (0.5–2.5 g.L⁻¹), pH (2–6) and initial metal ions concentration (30–110 mg.L⁻¹) along with the observed responses for removal of thorium(IV) have been shown in Table 3.

The second-order polynomial equation was used to find out the relationship between the variables and response. In this way, the regression equation coefficients were calculated and the data were fitted to a second-order polynomial equation. In order to check the acceptability of the model, the analysis of variance (ANOVA) was used for a removal study of Th(IV) ion with IR-120 and IRA-400 either discretely or in combination. The test for the significance of the regression model and the results of ANOVA are reported in Table 4. It must be mentioned that a Prob > F less than 0.05 indicate the significance of the model terms.

Three verification experiments were conducted for adsorption of Th(IV) ions onto a resin of IR-120 and IRA-400 and a mixture of both. To verify the accuracy of the data the corresponding correlation coefficient values (R^2) and adjusted R^2 values were obtained. The mentioned values in the case of using IR-120 are 0.9871 and 0.9755, in the case of IRA-400 are 0.9921 and 0.9850 and for a composite of both are 0.9943 and 0.9891, respectively. Due to the proximity of these

Table 3. Full factorial central composite design matrix of orthogonal and real values along with the observed responses for removal of thorium(IV).

Run order	Real (coded) values			Removal efficiency (%)					
	A	B	C	IR-120		IRA-400		IR-120+IRA-400	
				Experimental	Predicted	Experimental	Predicted	Experimental	Predicted
1	3(-1)	50(-1)	1(-1)	89.82	92.85	7.87	7.05	67.19	66.45
2	5(+1)	50(-1)	1(-1)	66.13	65.13	16.02	16.53	38.63	40.13
3	3(-1)	90(+1)	1(-1)	86.36	77.37	3.10	3.09	56.61	55.33
4	5(+1)	90(+1)	1(-1)	55.52	54.43	8.24	8.81	26.74	26.73
5	3(-1)	50(-1)	2(+1)	99.46	99.61	16.60	15.19	70.76	71.25
6	5(+1)	50(-1)	2(+1)	88.91	89.19	32.47	31.63	66.02	67.81
7	3(-1)	90(+1)	2(+1)	97.28	98.17	14.28	12.95	68.85	67.85
8	5(+1)	90(+1)	2(+1)	84.04	82.45	25.64	25.63	60.89	62.13
9	2(- α)	70(0)	1.5(0)	99.13	95.84	7.37	8.83	65.91	67.43
10	6(+ α)	70(0)	1.5(0)	47.37	49.96	31.40	30.89	37.37	35.39
11	4(0)	30(- α)	1.5(0)	98.23	96.74	20.75	21.63	70.31	69.05
12	4(0)	110(+ α)	1.5(0)	84.65	84.66	11.67	11.67	51.49	52.25
13	4(0)	70(0)	0.5(- α)	61.63	61.48	2.23	1.69	31.36	31.87
14	4(0)	70(0)	2.5(+ α)	99.29	98.64	25.29	26.65	72.11	71.07
15	4(0)	70(0)	1.5(0)	93.16	92.98	9.12	9.81	64.10	64.81
16	4(0)	70(0)	1.5(0)	93.06	92.98	9.73	9.81	64.94	64.81
17	4(0)	70(0)	1.5(0)	93.13	92.98	9.68	9.81	64.91	64.81
18	4(0)	70(0)	1.5(0)	93.33	92.98	10.11	9.81	65.35	64.81
19	4(0)	70(0)	1.5(0)	92.98	92.98	9.44	9.81	65.22	64.81
20	4(0)	70(0)	1.5(0)	93.71	92.98	9.92	9.81	64.84	64.81

Table 4. Analysis of variance (ANOVA) for Th(IV) removal by ion exchange resins.

Source	Sum of squares (coded)			DF	Prob>F		
	IR-120	IRA-400	R-120+IR-A400		IR-120	IRA-400	I-R120+IR-A400
Model	4541.04	1442.58	3666.32	9	<0.0001	<0.0001	<0.0001
A	2103.14	490.40	1027.36	1	<0.0001	<0.0001	<0.0001
B	145.68	99.30	281.82	1	0.0006	<0.0001	<0.0001
C	1379.75	623.50	1617.05	1	<0.0001	<0.0001	<0.0001
AB	12.10	7.07	2.57	1	0.1837	0.0325	0.2965
AC	118.12	24.29	261.40	1	0.0012	0.0010	<0.0001
BC	6.16	1.45	29.76	1	0.3323	0.2882	0.0038
A ²	632.75	157.11	282.97	1	<0.0001	<0.0001	<0.0001
B ²	8.14	73.18	27.18	1	0.2686	<0.0001	0.0050
C ²	261.76	30.07	258.43	1	<0.0001	0.0005	<0.0001
Residual	59.34	11.48	21.15	10			
Lack-of-fit	58.99	10.87	20.20	5	<0.0001	0.0034	0.0022
Pure error	0.35	0.62	0.95	5			

values to 1.0, it can be understood that a good agreement has been achieved between the correlated data and the experimental data. The final responses for the removal of Th(IV) ions using IR-120, IRA-400 and a composite of both of them (IR-120 and IRA-400) in terms of coded factors are reported in Eqs. (5-7):

$$\% \text{ Removal} = +92.98 - 11.47 \times A - 3.02 \times B + 9.29 \times C - 1.23 \times A \times B + 3.84 \times A \times C + 0.88 \times B \times C - 5.02 \times A^2 - 0.57 \times B^2 - 3.23 \times C^2 \quad (5)$$

$$\% \text{ Removal} = +9.81 + 5.54 \times A - 2.49 \times B + 6.24 \times C - 0.94 \times A \times B + 1.74 \times A \times C + 0.43 \times B \times C + 2.5 \times A^2 + 1.71 \times B^2 + 1.09 \times C^2 \quad (6)$$

$$\% \text{ Removal} = +64.81 - 8.01 \times A - 4.20 \times B + 10.05 \times C - 0.57 \times A \times B + 5.72 \times A \times C + 1.93 \times B \times C - 3.35 \times A^2 - 1.04 \times B^2 - 3.21 \times C^2 \quad (7)$$

where in these equations A, B and C are the coded terms for pH, initial Th(IV) concentration and adsorbent dosage, respectively.

3.2. Interaction effects of two variables

It is obvious that the sensitivity of the response to the two interacting variables can include three dimensional graphs by holding the other variable at the central values. On the basis of quadratic polynomial Eqs. (5-7) of the response surface methodology, the effects of interacting

variables were analyzed. The positive linear coefficient indicates that the Th(IV) removal percentage increased as the variable increased. Figure 1(a-c) shows the simultaneous effect of pH and initial metal ion concentration on Th(IV) removal efficiency in an aqueous solution with the resin of IR-120 (Figure 1a), IRA-400 (Figure 1b) and in combination (Figure 1c).

The 3-dimensional surface plot shows that the removal efficiency of Th(IV) for the three adsorbents was subject to changes in pH. According to Figures 1a and 1c, the removal efficiency of Th(IV) increased with pH ranging from 2.0 to 3.5, this phenomenon can be explained by the reduction of active sites of the adsorbent at low pH because of protonation of the functional groups. Moreover, at low pH the competition between Th⁴⁺ ions and hydrogen ions increases resulting in a decrease in removal efficiency. However, the removal efficiency of Th(IV) decreases when the pH is above 4.0, which can be due to the formation of different thorium species, such as [Th₂(OH)₂]⁶⁺, [Th₃(OH)₅]⁷⁺ and [Th₄(OH)₈]⁸⁺, which have a lower adsorption tendency [33,34]. The response plots show that the thorium removal efficiency firstly increases with an increase in the metal ions concentration and then decreases. The decrease in the percentage removal of metals ions can be attributed to the fact that all the adsorbents have a limited number of active sites, which are saturated above a certain initial metal ions concentration. Figure 1b shows that the removal efficiency of Th(IV) increases with an increase in pH from 2 to 6. It shows the ability of anionic resin to

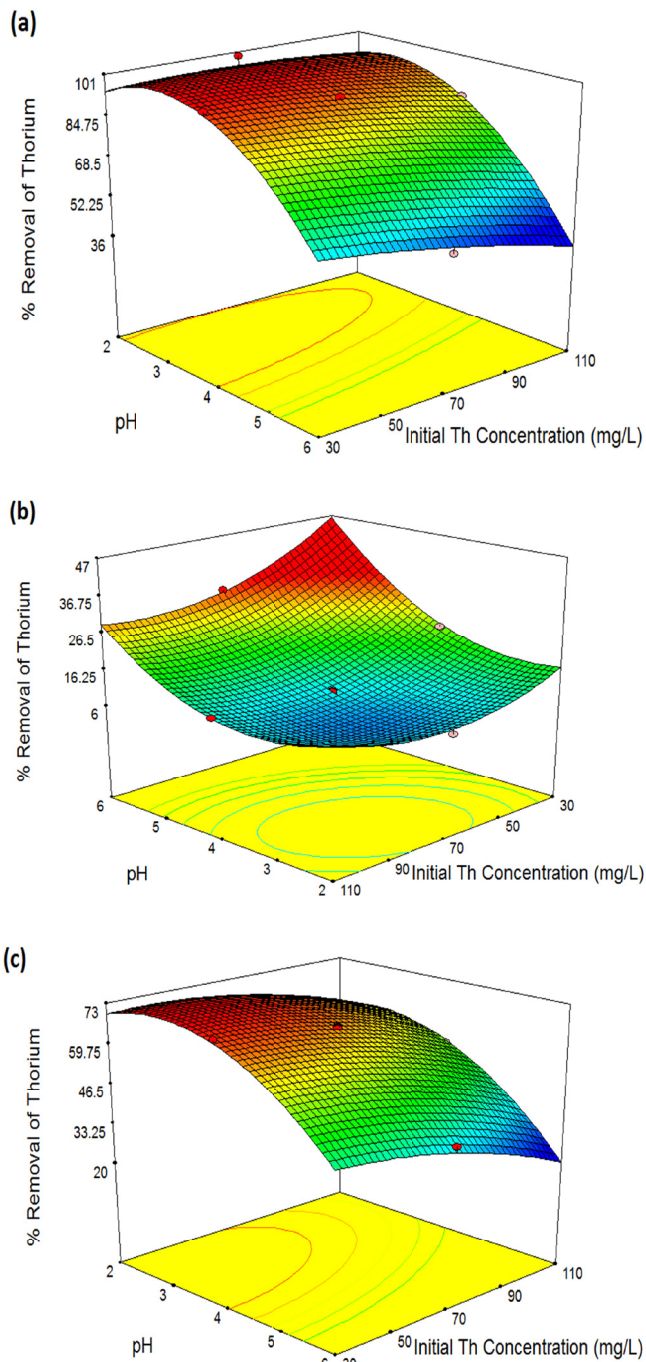


Fig. 1. Three-dimensional plots showing effect of initial Th(IV) ion concentration [mg.L⁻¹] and pH on the removal efficiency of Th(IV) using IR-120 (a), IRA-400 (b) and in combination (c), keeping adsorbent dosage 1.5 g.L⁻¹.

to remove thorium hydroxide is more than Th⁺⁴ ions. The three-dimensional response plots show the interactive effect of the pH and the adsorbent dosage (Figure 2).

In the case of using IR-120, it was proven that at an initial Th(IV) ion concentration of 70 mg.L⁻¹ and pH=4, the removal efficiency of Th(IV) increased from 61.63 to 99.29, and in the case of IRA-400 the same increased from 2.23 to 25.29. It was also proven that as the adsorbent dosage increased, the number of the

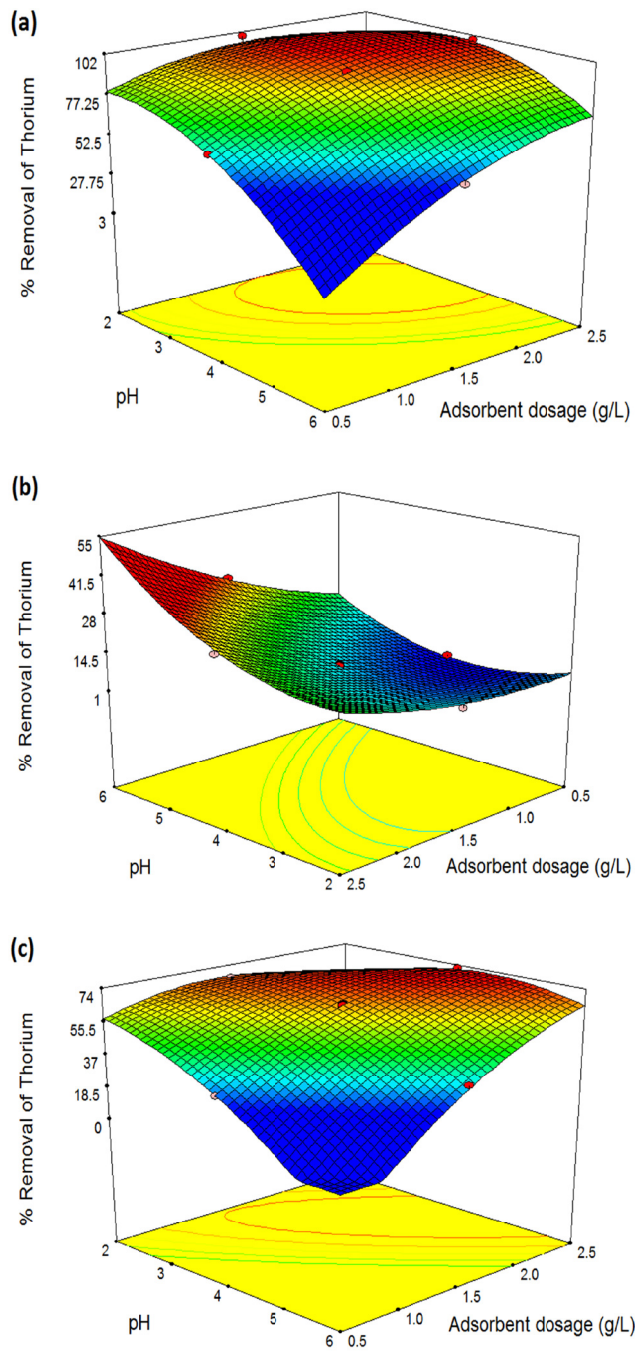


Fig. 2. Three-dimensional plots showing effect of pH and adsorbent dosage [mg.L⁻¹] on the removal efficiency of Th(IV) using IR-120 (a), IRA-400 (b) and in combination (c), keeping initial Th(IV) ion concentration 70 mg.L⁻¹.

unoccupied effective sites and the surface area also increased, improving the percentage of adsorption [35]. The interactive effects of the adsorbent dosage and initial Th(IV) ion concentration can be inferred from the response plot Figure 3(a-c), holding the pH equal to 4.

When the initial Th(IV) ion concentration increases from 30 to 110 mg.L⁻¹, the removal efficiency of Th(IV) decreases because of increasing driving force of the mass transfer and limited number of active sites on the

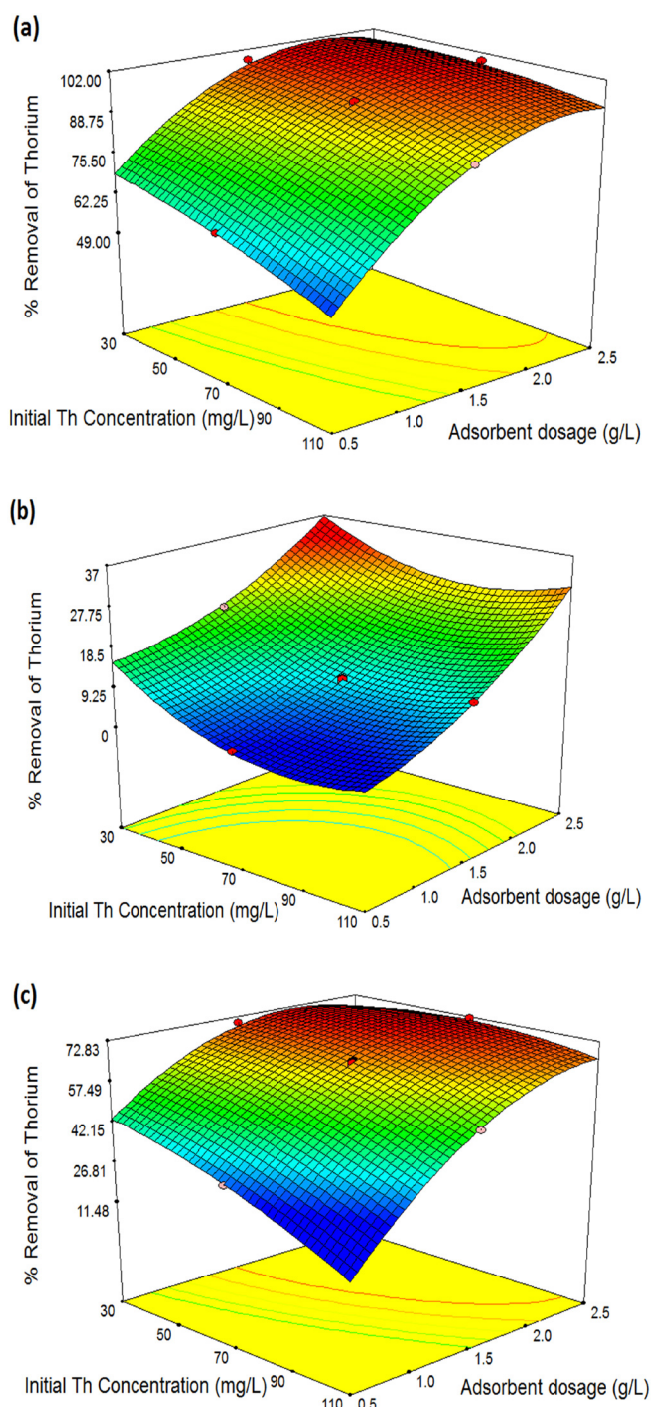


Fig. 3. Three-dimensional plots showing effect of initial Th(IV) ion concentration [$\text{mg}\cdot\text{L}^{-1}$] and adsorbent dosage [$\text{g}\cdot\text{L}^{-1}$] on the removal efficiency of Th(IV) using IR-120 (a), IRA-400 (b) and in combination (c), keeping pH 4.

and limited number of active sites on the adsorbent [36]. At the adsorbent dosage of $1.5 \text{ g}\cdot\text{L}^{-1}$, this is evidenced by greater removal efficiency of Th(IV) (98.23, 20.75 and 70.31) at initial Th(IV) ion concentrations of $30 \text{ mg}\cdot\text{L}^{-1}$ in comparison to 84.65, 11.67 and 51.49 at initial concentration of $110 \text{ mg}\cdot\text{L}^{-1}$ with IR-120, IRA-400 and a mix of the adsorbents, respectively. According to the P-value (>0.05) reported in Table 4, it can be seen

that the interaction between the resin dosage and the metal ion concentration for IR-120 and IRA-400 is not significant.

3.3 Optimization of Th(IV) removal

Optimization of the independent variables to maximize the removal efficiency of Th(IV) was performed using the quadratic model within the studied experimental range. The model optimization suggested the optimum values of the selected three independent process variables as; pH 3.23, 6 and 4.07; initial Th(IV) ion concentration of 78.2, 30.0 and $55.4 \text{ mg}\cdot\text{L}^{-1}$; and the adsorbent dose of 2.08, 2.5 and $2.2 \text{ g}\cdot\text{L}^{-1}$, to achieve the maximum reduction (99.82%, 66.31% and 73.15%) of the Th(IV) by resin of IR-120, IRA-400 and a mix of both as an adsorbent, respectively.

The removal efficiencies in specified conditions were obtained and then compared with the predicted values. As can be seen from Table 5, the percentage error between the removal efficiency of the experimental and predicted values was in the range of 0.70–4.39%. The experimental removal efficiency of Th(IV) onto resin of IR-120, IRA-400 and a mix of both, under optimum conditions was determined to be 98.09%, 63.52% and 72.19%, respectively. The reported errors showed that there is a good agreement between the experimental data and the predicted data using RSM.

3.4. Kinetic study

In this work, the adsorption of Th(IV) on Amberlite ion exchange resins is examined at different time intervals. Figure 4 shows the effect of time on the adsorption of Th(IV) at pH = 4, initial Th(IV) ion concentration of $70 \text{ mg}\cdot\text{L}^{-1}$ and adsorbent dosage of $1.5 \text{ g}\cdot\text{L}^{-1}$.

In this study, different kinetic models were tested to check the mechanism involved during the adsorption process, i.e. the pseudo-first order and the pseudo-second-order. The applicability of these kinetic models was determined by measuring the correlation coefficients (R^2) as well as the closeness of the experimental and calculated adsorption capacity values.

$$\text{Pseudo first-order: } q_t = q_e (1 - \exp(-k_1 t)) \quad (8)$$

$$\text{Pseudo second-order: } q_t = \frac{k_2 q_e^2 t}{1 + k_2 q_e t} \quad (9)$$

Table 5. Verification experiments for adsorption of Th(IV) ions onto resin of IR-120, IRA-400 and the mix of them.

Adsorbent	No.	Condition			Removal efficiency of Th(IV)		Error (%)
		pH	Initial concentration (mg.g ⁻¹)	Adsorbent dose (g.L ⁻¹)	Observed values	Predicted values	
IR-120	1	2	70	2	95.64	94.22	1.48
	2	3	50	2.5	97.70	96.87	0.85
	3	4	30	2.5	97.92	98.88	0.98
	Opt	3.23	78.2	2.08	98.09	99.82	1.76
IRA-400	1	5	50	2.5	40.89	42.45	3.81
	2	5	30	2	43.56	44.71	2.64
	3	6	50	2.5	60.33	59.91	0.70
	Opt	6	30	2.5	63.52	66.31	4.39
IR-120 + IRA-400	1	3	50	2.5	66.44	64.02	3.64
	2	4	50	2.5	70.79	71.37	0.82
	3	5	70	2	64.95	66.01	1.63
	Opt	4.07	55.4	2.2	72.19	73.15	1.33

where k_1 (min⁻¹) is the pseudo-first-order rate constant and k_2 (g.mg⁻¹.min⁻¹) is the pseudo second-order rate constant. q_t and q_e (mg.g⁻¹) are the amounts of Th(IV) adsorbed on the adsorbent at time t and in equilibrium, respectively. In Table 6 the parameters of the kinetic models and the correlation coefficient of the models are reported.

As can be found from Table 6, in the case of the pseudo-second order reaction the R^2 values were better than those of the pseudo-first order. Also the experimental q_e values were close to the q_e values obtained from the slope of the linear plot of t/q_t versus t suggesting that the experimental data fits well into the pseudo-second-order model system (Table 6). In this way, the adsorption procedure was supportive of the pseudo-second order equation, which showed that the adsorption involved in the chemical reaction incorporated the physical adsorption, in like manner [37].

3.5. Adsorption isotherms

The initial concentration plays an important role to

overcome all mass transfer resistances of metal ions in adsorption from an aqueous phase to a solid phase. The Langmuir adsorption isotherm suggests monolayer sorption on a homogeneous surface without any interaction between the adsorbed molecules; this model can be written as follows [38]:

$$q_e = \frac{q_m K_L C_e}{1 + K_L C_e} \quad (10)$$

where q_e (mg.g⁻¹) is the equilibrium metal ion concentration on the sorbent, C_e (mg.L⁻¹) is the equilibrium metal ion concentration in the solution, q_m (mg.g⁻¹) is the monolayer sorption capacity of the sorbent (mg.g⁻¹), and K_L is the Langmuir sorption constant (L.mg⁻¹) relating the free energy of sorption. A multilayer sorption with a heterogeneous energetic distribution of active sites can be accompanied by interactions between the adsorbed molecules which is proposed by the Freundlich isotherm model [39]:

$$q_e = K_F C_e^{1/n} \quad (11)$$

Table 6. Kinetic parameters for the adsorption of Th(IV) onto ion exchange resins.

Experimental q_e (mg.g ⁻¹)*	Pseudo-first order			Pseudo-second order		
	k_1 (min ⁻¹)×10 ⁻³	q_e (mg.g ⁻¹)	R^2	k_2 (g.mg ⁻¹ .min ⁻¹)×10 ⁻⁴	q_e (mg.g ⁻¹)	R^2
(a) 43.39	9.21	46.18	0.786	4.55	44.84	0.996
(b) 4.58	7.14	4.36	0.906	25.48	4.99	0.998
(c) 30.24	9.67	39.59	0.884	4.94	30.00	0.998

* Kind of adsorbent: (a) IR-120, (b) IRA-400 and (c) Mix of them

Where K_F is a constant relating the sorption capacity and $1/n$ is an empirical parameter relating the sorption intensity, which varies with the heterogeneity of the material. Table 7 shows the parameters of these isotherm models. The linearized Langmuir sorption isotherm is plotted in Figure 5. It was found that the metal ion removal mechanism is related to the initial metal ion concentration. In other words, adsorption of metal ion takes place at definite sites only when the metal ion concentration is low, but as the concentration is increased, the sites are saturated and the exchange sites are filled [40]. Based on the correlation coefficients (Table 7), the Langmuir equation gives a better fit for the experimental data than the Freundlich one for the adsorption of Th(IV). Langmuir isotherm suggests monolayer coverage of the thorium species on the surface of the resins. The $n > 1$ obtained in the Freundlich model depicts a favorable adsorption.

Table 7. Langmuir and Freundlich constants for the adsorption of Th(IV) onto ion exchange resins.

Isotherm model	Adsorbent		
	IR-120	IRA-400	IR-120 + IRA-400
Langmuir			
q_m (mg.g ⁻¹)	24.15	2.43	13.11
K_L (L.mg ⁻¹)	0.151	0.026	0.045
R^2	0.9903	0.9854	0.9916
Freundlich			
K_F (mg.g ⁻¹)	4.921	0.209	1.094
n	2.654	2.228	1.964
R^2	0.9486	0.9227	0.8892

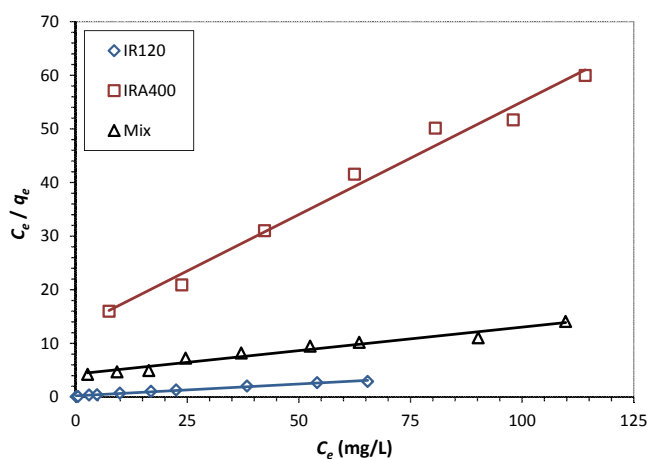


Fig 5. The Langmuir adsorption isotherm models of Th(IV) adsorption onto resins of IR-120, IRA-400 and the mix of them at $T = 25$ °C, $pH = 4$, adsorbent dose = 1.5 g.L⁻¹.

In Table 8 the maximum sorption capacity of Th(IV) ion onto the Amberlite IR-120Na⁺ is compared with that of the other adsorbents reported in the literature. As can be seen in Table 8, the maximum sorption capacity of Th(IV) ion onto the resin of IR-120 is in the same range of maximum sorption capacity of Th(IV) ion obtained by other researchers.

Table 8. Comparison of the various sorbents used for Th(IV) uptake.

Adsorbent	$q_{max, Th}$ (mg.g ⁻¹)	Ref.
XAD-4-o-phenylene dioxydiacetic acid	26.22	[39]
XAD-4-octacarboxymethyl-C-methyl calix resorcinaren	62.65	[40]
Merrifield chloromethylated resin-4-ethoxy-4-ethyl-N,N-bis-2-ethyl hexyl butanamide	46.41	[41]
PAN/zeolite	9.28	[42]
Crystalline tin oxide nanoparticles	62.5	[11]
Carboxylate-functionalised graft copolymer derived from titanium dioxide -densified cellulose	92.2	[43]
Amberlite IR-120Na ⁺	24.15	This work

3.6. FTIR analysis

In order to determine the main functional groups of the Amberlite IR-120 in Th(IV) adsorption, the infrared spectroscopy characteristics were compared before and after adsorption (Figure 6).

In Figure 6 the band at 2924 cm⁻¹ was attributed to C–H stretching vibrations. The intensive peak at 1633 cm⁻¹ was produced by C=O stretching vibration. The bands observed at 1413 cm⁻¹ assigned the stretching of the O–S–O group and at 836 cm⁻¹ presented the aromatic out of plane C–H band [41]. The comparison of FTIR spectra before and after adsorption of Th(IV) onto IR-120 shows that the intensities of the peak series in 1126 and 1035 cm⁻¹ regions were changed because of the metal complex formation between thorium ions and sulfonate groups of the resin [42]. The sulfonate (–SO₃⁻) groups band participating in ion exchange are located under 1035 – 1153 cm⁻¹ regions for the cationic resin.

The infrared spectroscopy of Amberlite IRA-400 is shown in Figure 7. The broad and strong band ranging from 3300 to 3600 cm⁻¹ might be due to –OH groups in both Figures 6 and 7.

The C=O stretching vibration is shown at 1629 and 1634 cm⁻¹ before and after adsorption, respectively. A

primary amine band can be seen at the range of 1440 to 1560 cm^{-1} and a secondary amine band is presented at the range of 1000 to 1350 cm^{-1} ; therefore, it can be concluded that there are two types of amines in the anionic resin. Furthermore, a peak at 1383 cm^{-1} is related to the NO_3^- functional group after adsorption of Th(IV) onto IRA-400.

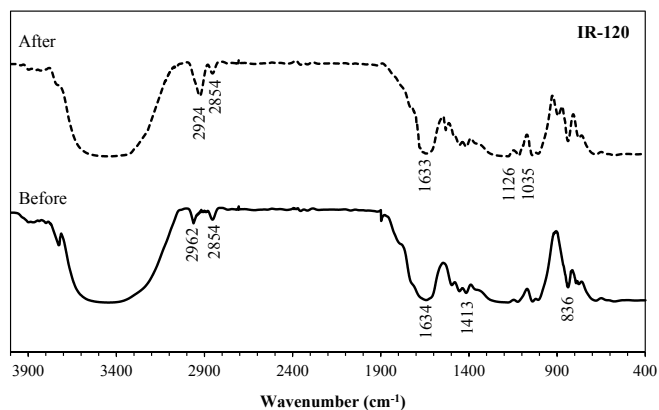


Fig. 6. FTIR spectra of the Amberlite IR-120 adsorbent before and after Th(IV) adsorption.

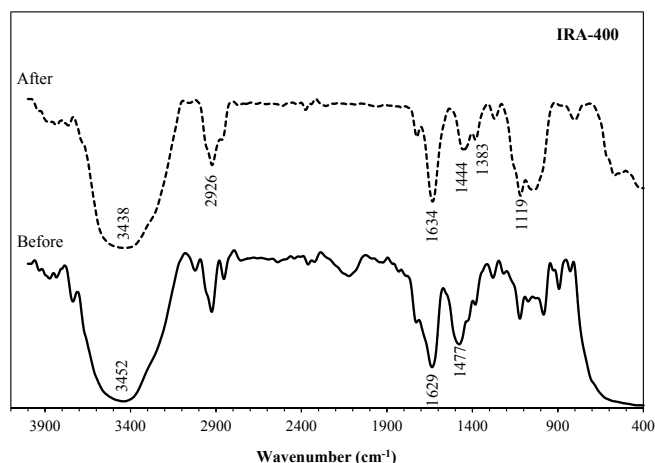


Fig. 7. FTIR spectra of the Amberlite IRA-400 adsorbent before and after Th(IV) adsorption.

4. Conclusion

The objective of this study was to explore the optimum process conditions via the response surface methodological approach, as required while using Amberlite IR-120, IRA-400 and a mix of both to remove thorium(IV) from the aqueous solutions. On the basis of the RSM approach using the central composite model for the experimental design and fitness of polynomial equation, maximum removal efficiencies of Th(IV) onto IR-120, IRA-400 and a mix of both with equal mass fraction were determined as 98.09%, 65.70% and 72.19% at pH of 3.23, 6 and 4.07, initial Th(IV)

concentration of 78.2, 30 and 55.4 mg.L^{-1} and the resin amount of 2.08, 2.5 and 2.2 g.L^{-1} , respectively.

The equilibrium adsorption data were correlated with Langmuir and Freundlich isotherm equations. The statistical parameters indicate that the Langmuir equation was the best fit and there was a good agreement between model and experimental data. The maximum monolayer adsorption capacities of Th(IV) onto IR-120, IRA-400 and a mix of both were found to be 24.15, 2.43 and 13.11 mg.g^{-1} , respectively. The kinetic of thorium adsorption was very well described by the pseudo-second-order kinetic model with R^2 values exceeding 0.996, 0.998 and 0.998 related to IR-120, IRA-400 and a mix of both, respectively. FTIR results showed that sulfonate groups were mainly involved in Th(IV) adsorption. Finally, Amberlite IR-120 Na^+ could be utilized successfully in the removal of thorium ion from aqueous solutions.

References

- [1] D.I. Ryabchikov, E.K. Gol'braikh, The Analytical Chemistry of Thorium, Pergamon Press, Oxford, 1963.
- [2] G.R. Choppin, Actinide speciation in the environment, *Radiochim. Acta*, 91 (2003) 645-650.
- [3] J.D. Van Horn, H. Huang, Uranium(VI) bio-coordination chemistry from biochemical, solution and protein structural data, *Coord. Chem. Rev.* 250 (2006) 765-775.
- [4] A.R. Keshtkar, M. Irani, M.A. Moosavian, Removal of uranium(VI) from aqueous solutions by adsorption using a novel electrospun PVA/TEOS/APTES hybrid nanofiber membrane: comparison with casting PVA/TEOS/APTES hybrid Membrane, *J. Radioanal. Nucl. Ch.* 295 (2013) 563-571.
- [5] M. Metaxas, V. Kasselouri-Rigopoulou, P. Galiatsatou, C. Konstantopoulou, D. Oikonomou, Thorium removal by different adsorbents, *J. Hazard. Mater.* 97 (2003) 71-82.
- [6] Z. Hongxia, D. Zheng, T. Zuyi, Sorption of thorium (IV) ions on gibbsite: effects of contact time, pH, ionic strength, concentration, phosphate and fulvic acid, *Colloid. Surface. A*, 278 (2006) 46-52.
- [7] A. Hamta, M.R. Dehghani, Application of polyethylene glycol based aqueous two-phase systems for extraction of heavy metals, *J. Mol. Liq.* 231 (2017) 20-24.

- [8] S. Chandramouleeswaran, J. Ramkumar, V. Sudarsan, A.V.R. Reddy, Boroaluminosilicate glasses: novel sorbents for separation of Th and U, *J. Hazard. Mater.* 198 (2011) 159-164.
- [9] J. Ramkumar, S. Chandramouleeswaran, V. Sudarsan, R.K. Vatsa, S. Shobha, V.K. Shrikhande, G.P. Kothiyal, T. Mukherjee, Boroaluminosilicate glasses as ion exchange materials, *J. Non-Cryst. Solids*, 356 (2010) 2813-2819.
- [10] A. Dyer, L.C. Jozefowicz, The removal of thorium from aqueous solutions using zeolites, *J. Radioanal. Nucl. Ch.* 159 (1992) 47-62.
- [11] L. Weijuan, T. Zuyi, Comparative study on Th(IV) sorption on alumina and silica from aqueous solutions, *J. Radioanal. Nucl. Ch.* 254 (2002) 187-192.
- [12] A. Nilchi, T. Shariati Dehaghan, S. Rasouli Garmarodi, Kinetics, isotherm and thermodynamics for uranium and thorium ions adsorption from aqueous solutions by crystalline tin oxide nanoparticles, *Desalination*, 321 (2013) 67-71.
- [13] S. Abbaszadeh, A.R. Keshtkar, M.A. Mousavian, Preparation of a novel electrospun polyvinyl alcohol/titanium oxide nanofiber adsorbent modified with mercapto groups for uranium(VI) and thorium(IV) removal from aqueous solution, *Chem. Eng J.* 220 (2013) 161-171.
- [14] J.S. Kentish, G.W. Stevens, Innovations in separation technology for the recycling and re-use of liquid waste streams, *Chem. Eng. J.* 84 (2001) 149-159.
- [15] A.A. Khan and R.P. Singh, Adsorption thermodynamics of carbofuran on Sn (IV) arsenosilicate in H^+ , Na^+ and Ca^{2+} forms, *Colloid. Surface. A*, 24 (1987) 33-42.
- [16] C.H. Lee, J.S. Kim, M.Y. Suh, W. Lee, A chelating resin containing 4-(2-thiazolylazo) resorcinol as the functional group synthesis and sorption behaviours for trace metal ions, *Anal. Chim. Acta*, 339 (1997) 303-312.
- [17] J.P. Rawat, K.P.S. Muktaawat, Thermodynamics of ion-exchange on ferric antimonite, *J. Inorg. Nucl. Chem.* 43 (1981) 2121-2128.
- [18] D.C. Sherrington, Preparation, structure and morphology of polymer supports, *Chem. Commun.* 21 (1998) 2275-2286.
- [19] J.H. Song, K.H. Yeon, S.H. Moon, Effect of current density on ionic transport and water dissociation phenomena in a continuous electrodeionization (CEDI), *J. Membrane Sci.* 291 (2007) 165-171.
- [20] J.S. Park, J.H. Song, K.H. Yeon, S.H. Moon, Removal of hardness ion from tap water using electromembrane processes, *Desalination*, 202 (2007) 1-8.
- [21] H.J. Lee, M.K. Hong, S.H. Moon, A feasibility study on water softening by electrodeionization with the periodic polarity change, *Desalination*, 284 (2012) 221-227.
- [22] T. Ho, A. Kurup, T. Davis, J. Hestekin, Wafer chemistry and properties for ion removal by wafer enhanced electrodeionization, *Sep. Sci. Technol.* 45 (2010) 433-446.
- [23] K. Dermentzis, Continuous electrodeionization through electrostatic shielding, *Electrochim. Acta*, 53 (2008) 2953-2962.
- [24] B.N. Singh, B. Maiti, Separation and pre-concentration of U(VI) on XAD-4 modified with 8-hydroxy quinoline, *Talanta*, 69 (2006) 393-396.
- [25] S. Chandramouleeswaran, Jayshree Ramkumar, n-Benzoyl-n-phenylhydroxylamine impregnated Amberlite XAD-4 beads for selective removal of thorium, *J. Hazard. Mater.* 280 (2014) 514-523.
- [26] A. Demirbas, E. Pehlivan, F. Gode, T. Altun, G. Arslan, Adsorption of Cu(II), Zn(II), Ni(II), Pb(II) and Cd(II) from aqueous solution on Amberlite IR-120 synthetic resin, *J. Colloid Interf. Sci.* 282 (2005) 20-25.
- [27] F. Semnani, Z. Asadi, M. Samadfam, H. Sepehrian, Uranium(VI) sorption behavior onto amberlite CG-400 anion exchange resin: Effects of pH, contact time, temperature and presence of phosphate, *Ann. Nucl. Energy*, 48 (2012) 21-24.
- [28] S. Rengaraj, K.H. Yeon, S.Y. Kang, J.U. Lee, K.W. Kim, S.H. Moon, Studies on adsorptive removal of Co(II), Cr(III) and Ni(II) by IRN77 cation-exchange resin, *J. Hazard. Mater.* 92 (2002) 185-198.
- [29] M. Singh, A. Sengupta, Sk. Jayabun, T. Ippili, Understanding the extraction mechanism, radiolytic stability and stripping behavior of thorium by ionic liquid based solvent systems: evidence of ion-exchange and solvation mechanism, *J. Radioanal. Nucl. Ch.* 311 (2017) 195-208.
- [30] M. Elibol, D. Ozer, Response surface analysis of lipase production by freely suspended *Rhizopus arrhizus*, *Process Biochem.* 38 (2002) 367-372.
- [31] M. Gavrilescu, Removal of heavy metals from the environment by biosorption, *Eng. Life Sci.* 4 (2004) 219-232.

- [32] F. Ghorbani, H. Younesi, S.M. Ghasempouri, A.A. Zinatizadeh, M. Amini, A. Daneshi, Application of response surface methodology for optimization of cadmium biosorption in an aqueous solution by *saccharomyces serevisiae*, *Chem. Eng. J.* 145 (2008) 267-275.
- [33] V.K. Gupta, B. Gupta, A. Rastogi, S. Agarwal, A. Nayak, A comparative investigation on adsorption performances of mesoporous activated carbon prepared from waste rubber tire and activated carbon for a hazardous azo dye-Acid Blue 113, *J. Hazard. Mater.* 186 (2011) 891-901.
- [34] V.K. Gupta, A. Mittal, A. Malviya, and J. Mittal, Adsorption of carmoisine a from waste materials-bottom ash and deoiled soya, *J. Colloid. Interface Sci.*, 355 (2009) 24–33.
- [35] T.S. Anirudhan, S. Jalajamony, Ethylthio-semicarbazide intercalated organophilic calcined hydrotalcite as a potential sorbent for the removal of uranium(VI) and thorium(IV) ions from aqueous solutions, *J. Env. Sci.* 25 (2013) 717-725.
- [36] G.H. Mirzabe, A.R. Keshtkar, Application of response surface methodology for thorium adsorption on PVA/Fe₃O₄/SiO₂/APTES nanohybrid adsorbent, *J. Ind. Eng. Chem.* 26 (2015) 277-285.
- [37] T.S. Anirudhan, S. Rijith, A.R. Tharun, Adsorptive removal of thorium(IV) from aqueous solution using poly (methacrylic acid)-grafted chitosan/bentonite composite matrix: Process design and equilibrium studies, *Colloid. Surface. A*, 368 (2010) 13-22.
- [38] I. Langmuir, The constitution and fundamental properties of solids and liquids. part I. solids, *J. Am. Chem. Soc.* 38 (1916) 2221-2295.
- [39] Y.S. Ho, G. Mckay, Pseudo-second order model for sorption processes, *Process Biochem.* 34 (1999) 451-465.